A Study of the Resistivity Method Using a Resistance Network Analyzer

By

Eizaburo YOSHIZUMI* and Tsuneji IRIE*

(Received October 31, 1961)

In the engineering field, many problems arise which are solved by Laplace's equation. These problems such as gravitation, electrostatics, magnetics, heat transfer and fluid mechanics, can be solved approximately by use of a resistance network analyzer.

In the present paper, the authors discuss the resistivity method with such an analyzer which has been applied to the investigation of electrical prospecting by the authors and their assistants since 1954[1].

It is shown that the resistivity curves obtained with this analyzer agree with the curves calculated theoretically, so that the authors are sure that this method of determining the resistances of boundaries is satisfactory, and that this analyzer will be an indispensable instrument in the solution of resistivity problems that can not be solved theoretically.

1. Laplace's equation for a two dimensional resistance network analyzer[2]

Portions of the two dimensional resistance network are shown in Fig. 1. Typical junctions are presented in Fig. 2. V_0, V_1, V_2, $\cdots$ are voltages at points

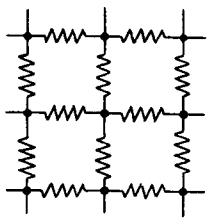

Fig. 1. Portions of the two dimensional resistance network.

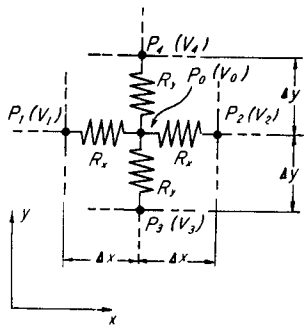

Fig. 2. Junctions of resistors.

P_0, P_1, P_2, $\cdots$. Applying Kirchhoff's law to the node P_0, we obtain

$$\frac{V_1-V_0}{R_x}+\frac{V_2-V_0}{R_x}+\frac{V_3-V_0}{R_y}+\frac{V_4-V_0}{R_y}=0, \tag{1.1}$$

and then we get

* Department of Mining Engineering.

$$\frac{1}{R_x}(V_1+V_2-2V_0)+\frac{1}{R_y}(V_3+V_4-2V_0)=0. \tag{1.2}$$

If there is the following relation

$$\frac{R_x}{R_y}=\left(\frac{\Delta x}{\Delta y}\right)^2, \tag{1.3}$$

inserting eq. (1.3) into eq. (1.2), we get

$$\frac{1}{\Delta x^2}(V_1+V_2-2V_0)+\frac{1}{\Delta y^2}(V_3+V_4-2V_0)=0. \tag{1.4}$$

Eq. (1.4) is the potential equation at the node of the resistance network.

On the other hand, Laplace's two dimensional equation is

$$\frac{\partial^2 v}{\partial x^2}+\frac{\partial^2 v}{\partial y^2}=0. \tag{1.5}$$

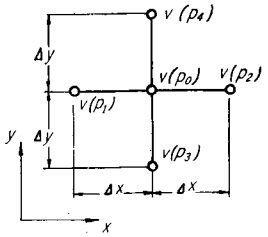

Fig. 3. Portions of the infinite medium.

Portions of the two dimensional infinite medium are shown in Fig. 3. $v(p_0)$, $v(p_1)$, $v(p_2)$, ⋯ are voltages at points p_0, p_1, p_2, ⋯.

Applying Taylor's expansion theorem to the x axis, we obtain $v(p_1)$ and $v(p_2)$:

$$\left.\begin{aligned} v(p_1) &= v(p_0)-\Delta x\left(\frac{\partial v}{\partial x}\right)_{p_0}+\frac{\Delta x^2}{2!}\left(\frac{\partial^2 v}{\partial x^2}\right)_{p_0}-\cdots \\ v(p_2) &= v(p_0)+\Delta x\left(\frac{\partial v}{\partial x}\right)_{p_0}+\frac{\Delta x^2}{2!}\left(\frac{\partial^2 v}{\partial x^2}\right)_{p_0}+\cdots \end{aligned}\right\}. \tag{1.6}$$

From eq. (1.6), ignoring terms of more than the 3rd order, we get

$$\left(\frac{\partial^2 v}{\partial x^2}\right)_{p_0}=\frac{1}{\Delta x^2}\{v(p_1)+v(p_2)-2v(p_0)\}. \tag{1.7}$$

In a similar manner we obtain the following equation about the y axis:

$$\left(\frac{\partial^2 v}{\partial y^2}\right)_{p_0}=\frac{1}{\Delta y^2}\{v(p_3)+v(p_4)-2v(p_0)\}. \tag{1.8}$$

From eqs. (1.7) and (1.8), we get

$$\left(\frac{\partial^2 v}{\partial x^2}\right)_{p_0}+\left(\frac{\partial^2 v}{\partial y^2}\right)_{p_0}=\frac{1}{\Delta x^2}\{v(p_1)+v(p_2)-2v(p_0)\}+\frac{1}{\Delta y^2}\{v(p_3)+v(p_4)-2v(p_0)\}. \tag{1.9}$$

Therefore, it can be shown that the voltages of the resistance network approximately satisfy Laplace's equation.

2. Resistors in the vicinity of the boundaries

The simplest method is to approximate an irregular boundary with a jagged

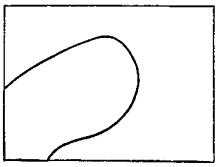

Fig. 4. An irregular boundary.

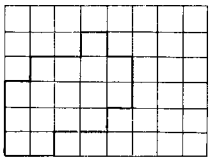

Fig. 5. A jagged line.

line, just as the irregular boundary of Fig. 4 is represented by the jagged line of Fig. 5. In this case, the smaller the net spacing the smaller the error but the greater the number of resistors needed. In this paper, the authors intend to discuss an approximate method for representing a boundary with a reasonable number of resistors.

2.1 Boundaries in the earth

We determine the value of the resistor in Fig. 6, where the boundary MN is parallel to the x axis, and divides the medium into resistivities ρ_1 and ρ_2.

The resistance $(R_{AB})_{\rho_1}$ attributed by ρ_1 is

$$(R_{AB})_{\rho_1} = \rho_1 \frac{\Delta x}{n\Delta y}, \tag{2.1}$$

and the resistance $(R_{AB})_{\rho_2}$ by ρ_2 is

$$(R_{AB})_{\rho_2} = \rho_2 \frac{\Delta x}{(1-n)\Delta y}, \tag{2.2}$$

and then we obtain R_{AB} as follows:

$$R_{AB} = \frac{\rho_1\rho_2}{(1-n)\rho_1+n\rho_2} \cdot \frac{\Delta x}{\Delta y}. \tag{2.3}$$

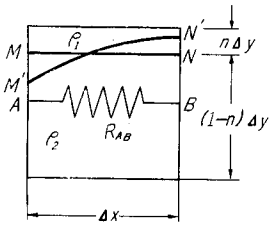

Fig. 6. Determining the value of resistors.

In the case of a boundary M′N′ (see Fig. 6), using MN for M′N′, where the area AM′N′B equals the area AMNB, we get the above equation.

We determine the resistance R_{AB} in Fig. 7, where the boundary is M′N′, which divides the medium into resistivities ρ_1 and ρ_2. In this case, the resistance $(R_{AB})_{\rho_1}$ by ρ_1 only is

$$(R_{AB})_{\rho_1} = \rho_1 \frac{\alpha\Delta x}{\Delta y}, \tag{2.4}$$

and the resistance $(R_{AB})_{\rho_2}$ by ρ_2 only is

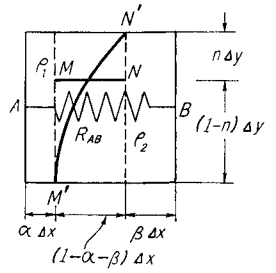

Fig. 7. Determining the value of R_{AB}.

$$(R_{AB})_{\rho_2} = \rho_2 \frac{\beta \Delta x}{\Delta y}, \tag{2.5}$$

and the resistance $(R_{AB})_{\rho_1, \rho_2}$ by ρ_1 and ρ_2 is

$$(R_{AB})_{\rho_1, \rho_2} = \frac{\rho_1 \rho_2 (1-\alpha-\beta)}{(1-n)\rho_1 + n\rho_2} \cdot \frac{\Delta x}{\Delta y}. \tag{2.6}$$

The resistance R_{AB} is a series combination of the above three resistances $(R_{AB})_{\rho_1}$, $(R_{AB})_{\rho_2}$ and $(R_{AB})_{\rho_1, \rho_2}$, and then we get,

$$R_{AB} = \left\{ \alpha\rho_1 + \beta\rho_2 + \frac{(1-\alpha-\beta)\rho_1\rho_2}{(1-n)\rho_1 + n\rho_2} \right\} \cdot \frac{\Delta x}{\Delta y}. \tag{2.7}$$

If $\rho_1 = \rho_2 = \rho_0$, from eq. (2.7), we get

$$R_{AB} = \rho_0 \frac{\Delta x}{\Delta y}. \tag{2.8}$$

From eq. (2.8), it is easily shown that eq. (1.3) is satisfied, as we had previously assumed.

The authors call the above method the equivalent vector area method.

2.2 Boundaries on the surface

When we use the resistivity method, we usually measure potentials on the surface and then calculate carefully the value of the resistor corresponding to a boundary on the surface, in order to avoid the topographic effect.

A portion of such a boundary is illustrated in Fig. 8, where the curve AB is the boundary between the atmosphere and the ground. By assuming ABCD,

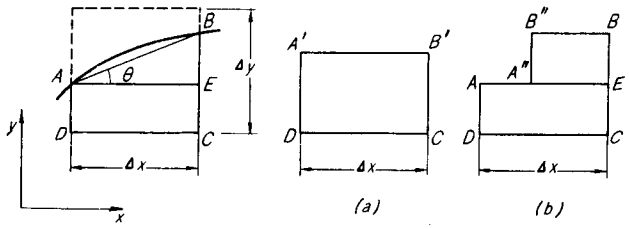

Fig. 8. Determining the value of R_{AB}.

which has a resistivity ρ_0 and is surrounded by infinite resistivity, we can determine the value of R_{AB}, R_{CB}, R_{DC} and R_{DA}.

The area ABCD can be represented by Figs. 8 (a) and 8 (b).

From Fig. 8 (a), we get

$$R_{A'B'} = R_{DC} = 2\rho_0 \frac{DC}{A'D}, \tag{2.9}$$

and from Fig. 8 (b), we get

$$R_{AD} = R_{EC} = 2\rho_0 \frac{AD}{DC}, \tag{2.10}$$

and

$$R_{A''B''} = R_{BE} = 2\rho_0 \frac{BE}{A''E}. \tag{2.11}$$

The resistance R_{AB} is obtained by the projection of resistances $R_{A'B'}$ and $R_{A''B''}$ as follows,

$$R_{AB} = 2\rho_0 \left(\frac{DC}{A'D} \cos\theta + \frac{BE}{A''E} \sin\theta \right). \tag{2.12}$$

When ABCD is surrounded by the finite resistivity, resistances R_{DC}, R_{AD} and R_{BC} are determined by a parallel combination of their adjacent resistances which in turn are determined in a similar manner.

The authors call the above method the equivalent vector area projection method.

3. Examples having boundaries in the earth

In this section, the authors explain the resistivity curves obtained by the resistance network analyzer using the equivalent vector area method. The curves are compared with the ones obtained theoretically.

3.1 Buried cylinder (I)

In case of this example the theoretical calculation is very troublesome. On the contrary, the resistivity curves are measured by the analyzer with ease.

This example is shown in Fig. 9, where the radius r is represented by the net spacing and the distance s from the surface to the center is 1.5 times as large as the net spacing. In Fig. 9 (a), the center of the cylinder lies on the mid-point of the resistor, and in Fig. 9 (b), the center of the cylinder does not lie on the resistor.

The values of the resistors are shown in Table 1, of which the resistances are shown in Fig. 10, where the unit of resistance is kΩ and the value indicated by a single bar (—) is 1 kΩ and the value indicated by a double bar (=) is 2 kΩ. The ratios of ρ_2 (the resistivities inside the cylinder) to ρ_1 (the resistivities outside the cylinder) are ∞, 10, 5, 2, 0.5, 0.2, 0.1 and 0 respectively.

The resistivity curves measured by the analyzer are shown in Fig. 11, where the black dots (●) and the white dots (○) represent the values measured by Figs. 10 (a) and 10 (b) respectively, using the equi-spacing four electrode method, of which the spacing is a.

Table 1. The values of resistors.

R (kΩ) \ ρ_2/ρ_1	∞	10	5	2	0.5	0.2	0.1	0
R_1	∞	4.50	2.62	1.43	0.76	0.61	0.55	0.50
R_2	5.97	3.86	2.87	1.65	0.56	0.25	0.13	0
R_3	1.05	1.04	1.03	1.00	0.91	0.82	0.79	0.63
R_4	∞	10.0	5.00	2.00	0.50	0.20	0.10	0
R_5	1.85	1.70	1.57	1.29	0.68	0.35	0.19	0
R_6	1.75	1.63	1.47	1.21	0.81	0.64	0.57	0.50
R_7	25.0	7.40	4.30	1.92	0.51	0.21	0.10	0

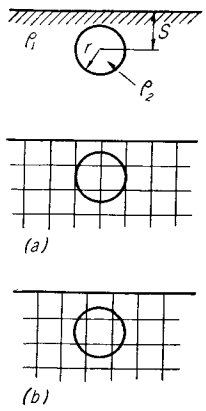

Fig. 9. A buried cylinder (I).

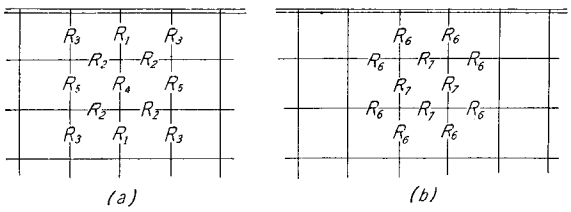

Fig. 10. Resistances.

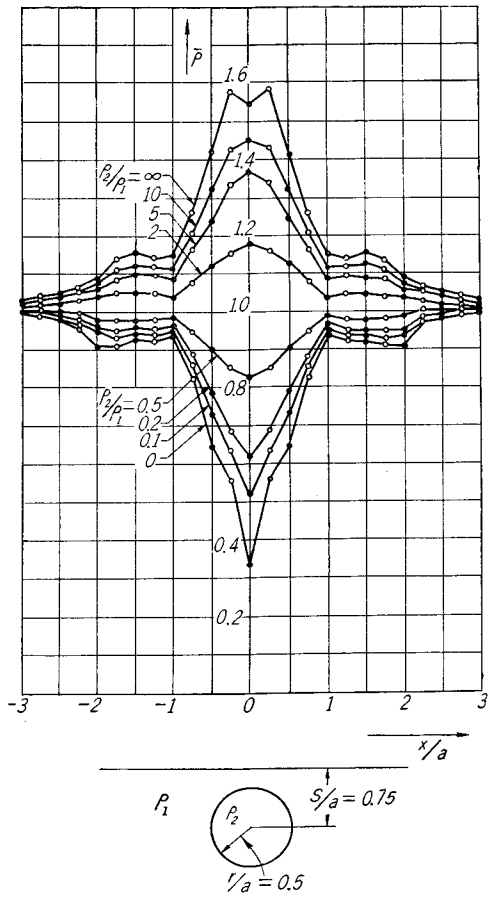

Fig. 11. Resistivity curves.

3.2 Buried cylinder (II)

This example is shown in Fig. 12, where the length of the radius and the distance from the surface to the center are both represented by the net spacing. In Fig. 12 (a), the center of the cylinder lies on the node of the resistors, and in Fig. 12 (b), the center of the cylinder lies on the mid-point of the resistor.

The values of the resistors are shown in Table 2, of which the resistances are shown in Fig. 13. The ratios ρ_2 (the resistivities inside the cylinder) to ρ_1 (the resistivities outside the cylinder) are ∞, 10, 5, 2, 0.5, 0.2, 0.1 and 0 respectively.

Table 2. The values of resistors. When $\rho_2/\rho_1=\infty$, the two resistors indicated by R_1 are not connected with each other.

R (kΩ) \ ρ_2/ρ_1	∞	10	5	2	0.5	0.2	0.1	0
R_1	6.05	4.95	4.20	2.93	1.28	0.72	0.50	0.27
R_2	∞	9.00	4.67	1.93	0.51	0.21	0.10	0
R_3	1.47	1.39	1.33	1.18	0.78	0.49	0.34	0.13
R_4	∞	11.6	7.57	3.70	1.04	0.43	0.22	0
R_5	2.21	2.16	2.12	2.01	1.72	1.52	1.39	1.27
R_6	5.97	3.86	2.87	1.65	0.56	0.25	0.13	0
R_7	∞	10.0	5.00	2.00	0.50	0.20	0.10	0
R_8	∞	4.50	2.62	1.43	0.76	0.61	0.55	0.50
R_9	1.85	1.70	1.57	1.29	0.68	0.35	0.19	0
R_{10}	1.05	1.04	1.03	1.00	0.91	0.82	0.76	0.63

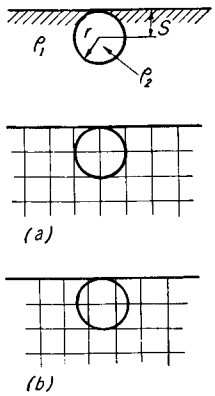

Fig. 12. A buried cylinder (II).

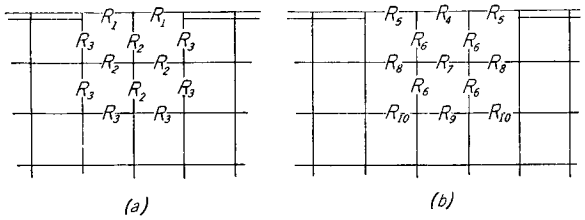

Fig. 13. Resistances.

The resistivity curves measured by the analyzer are shown in Fig. 14 where the black dots (●) and the white dots (○) represent the values measured by Figs. 12 (a) and 12 (b) respectively, using the equi-spacing four electrode method.

The theoretical resistivity curves which were calculated by Takeshi Kiyono

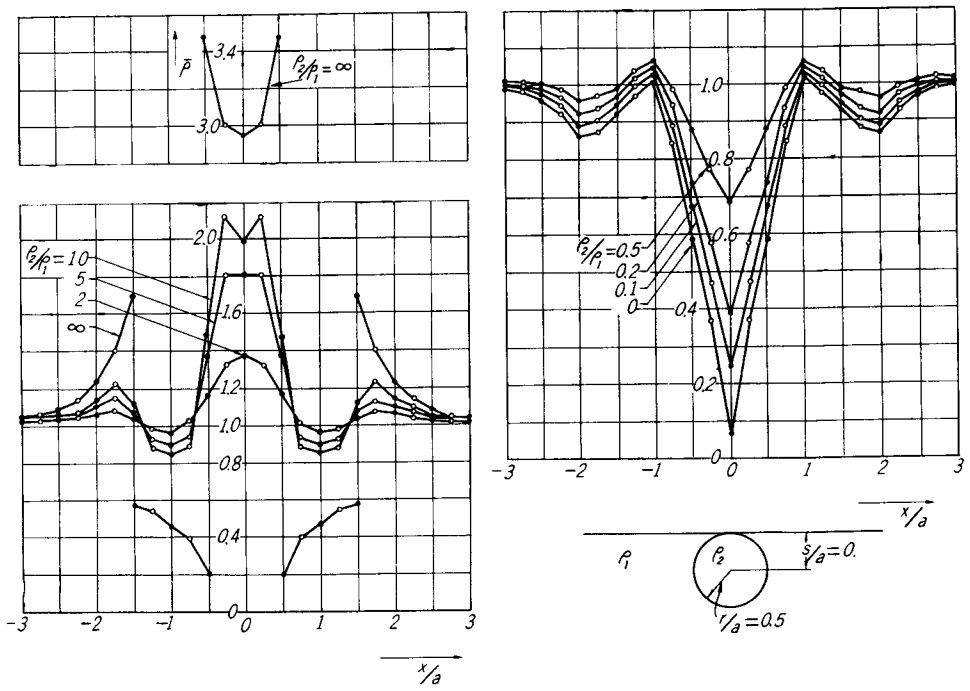

Fig. 14. Resistivity curves.

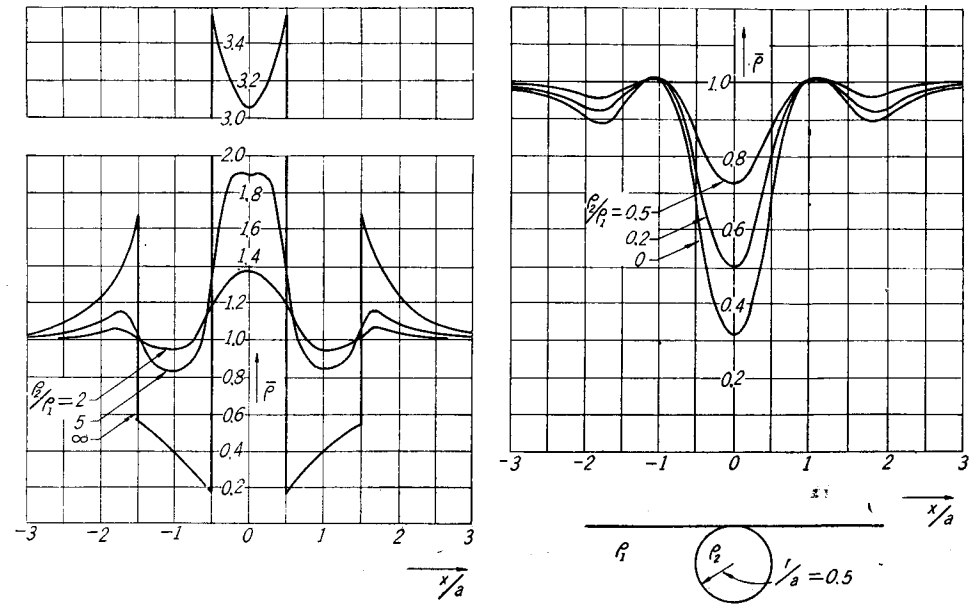

Fig. 15. Theoretical resistivity curves.

of Kyoto University are shown in Fig. 15[3].

In these examples, we see that the curves obtained by the analyzer agree with the ones obtained theoretically and are thereby assured that the equivalent vector area method is valid.

It is clear that the error introduced by the analyzer at the boundary may be kept within acceptable limits, by making the net spacing sufficiently small.

4. Examples having boundaries on the surface

In this section, the authors explain the resistivity curves obtained by the resistance network analyzer using the equivalent vector area projection method. The curves are compared with the ones obtained theoretically.

4.1 Protuberance of the semi-circular plate section (I)

There is a protuberance of the semi-circular plate section of which the radius r (as shown in Fig. 16) is represented by twice the net spacing. When the center of the cylinder lies on the node of the resistance network, the values of the resistors are shown in Fig. 17 (a), and when the center lies on the mid-point

Fig. 16. A protuberance of the semi-circular plate section.

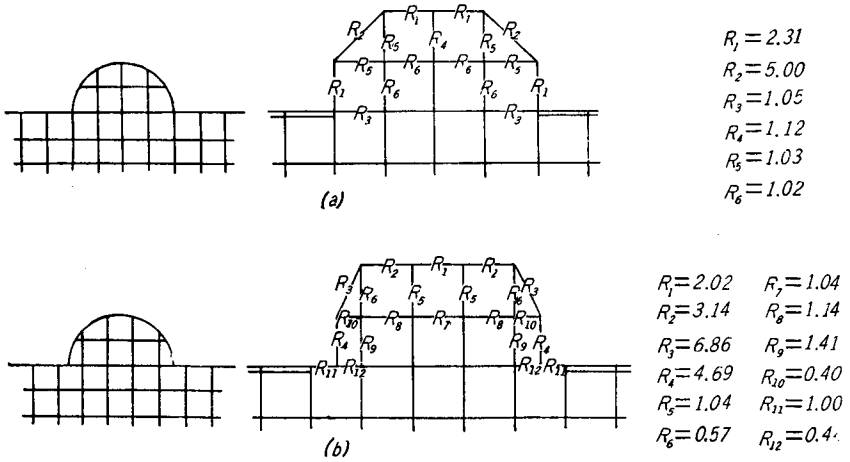

$R_1 = 2.31$
$R_2 = 5.00$
$R_3 = 1.05$
$R_4 = 1.12$
$R_5 = 1.03$
$R_6 = 1.02$

$R_1 = 2.02$ $R_7 = 1.04$
$R_2 = 3.14$ $R_8 = 1.14$
$R_3 = 6.86$ $R_9 = 1.41$
$R_4 = 4.69$ $R_{10} = 0.40$
$R_5 = 1.04$ $R_{11} = 1.00$
$R_6 = 0.57$ $R_{12} = 0.4$

Fig. 17. Center positions and valves of the resistors.

between the nodes, the values of the resistors are shown in Fig. 17 (b). In Figs. 17 (a) and 17 (b), the unit of resistance is the kΩ and the value indicated by a single bar (——) is 1 kΩ and the value indicated by a double bar (═══) is 2 kΩ.

The resistivity curves measured by the resistance network analyzer using the equi-spacing four electrode method, are shown in Fig. 18, where the black dots (●) are the values measured by Fig. 17 (a) and the white dots (○) are the values measured by Fig. 17 (b). In Fig. 18, a is the spacing between the electrodes, and r and x are indicated by taking a as the standard unit.

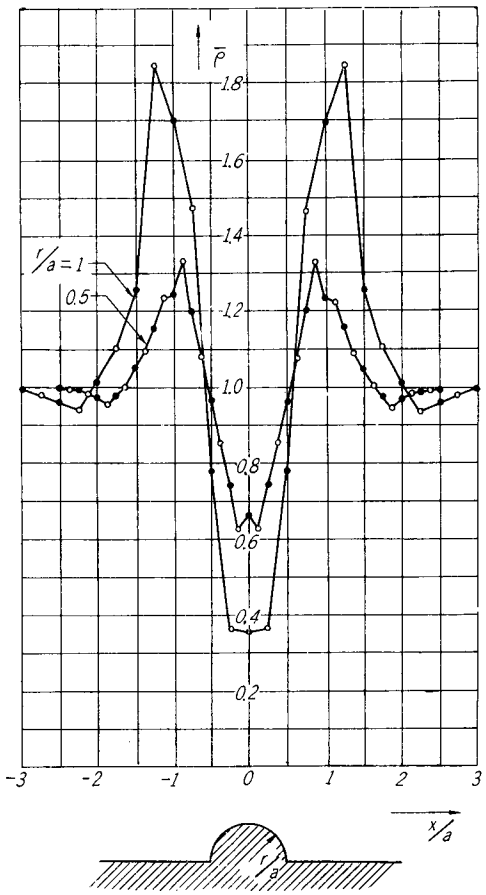

Fig. 18. Resistivity curves.

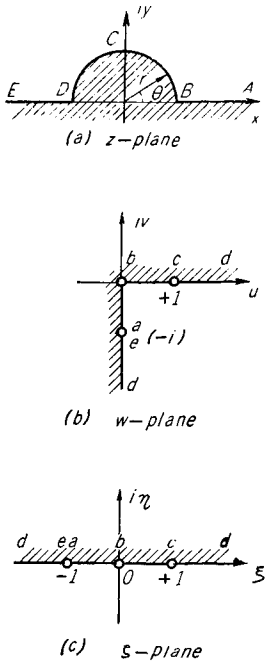

Fig. 19. (a) : z-plane, (b) : w-plane, (c) : ζ-plane.

The authors calculated the potentials theoretically.

First of all, we must transform the domain of the z-plane (Fig. 19 (a)) into the w-plane (Fig. 19 (b)). The transformation is given by the following equation,

$$w = -i\frac{z-r}{z+r}, \tag{4.1}$$

where

$$0 < arg\, w < \frac{3}{2}\pi . \qquad (4.2)$$

Points B($z=+r$), C($z=i$) and D($z=-r$) correspond to points $b(w=0)$, $c(w=+1)$ and $d(w=\infty)$ respectively and the infinite point ($z=\infty$) corresponds to the point ($w=-i$).

Next, we must transform the domain of the w-plane (Fig. 19 (b)) into the ζ-plane (Fig. 19 (c)). This transformation is given by the following equation,

$$w = \zeta^{3/2} . \qquad (4.3)$$

Both axes AB and DE correspond to the negative ξ axis, and the arc BCD corresponds to the positive ξ axis and these relations are given as follows,

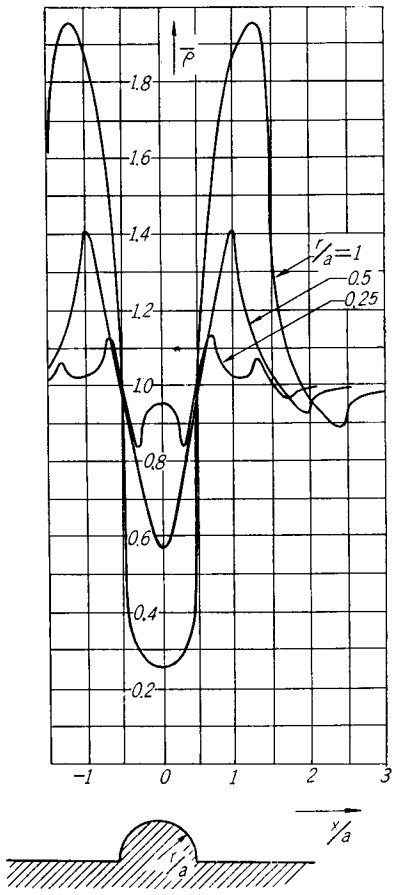

Fig. 20. Theoretical resistivity curves.

$$\left.\begin{aligned} &A \to B, \quad \xi = -v^{2/3} = -\left(\frac{x-r}{x+r}\right)^{2/3}, \quad x > +r, \\ &B \to D, \quad \xi = \tan^{3/2}\frac{\theta}{2}, \quad x = r\cos\theta, \quad 0 < \theta < \pi, \\ &D \to E, \quad \xi = -v^{2/3} = -\left(\frac{-x+r}{-x-r}\right)^{2/3}, \quad x < -r . \end{aligned}\right\} \qquad (4.4)$$

The resistivity curves calculated by the ζ-plane are shown in Fig. 20.[4]

Comparing Fig. 18 with Fig. 20, the authors are sure that the equivalent vector area projection method is settled satisfactorily.

4.2 Protuberance of the semi-circular section (II)

We discuss the case in which the radius of the semi-circular section equals the net spacing, in order to check the effect of coarse grids. It is expected that the resistivity curves obtained with the analyzer differ from the theoretical ones.

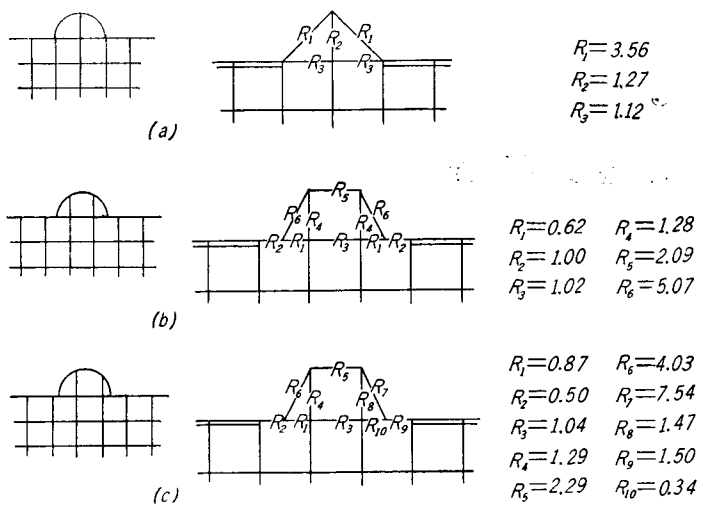

Fig. 21. Center positions and values of the resistors.

Figs. 21 (a), 21 (b) and 21 (c) show the three different center positions of the semi-circular plate, namely, in Fig. 21 (a), the center lies on the node and, in Fig. 21 (b), the center lies on the mid-point between the nodes, and in Fig. 21 (c), the center lies on the mid-point between the two center positions above.

The values of the resistors are shown in their figures respectively. From these cases we obtain the resistivity curves as shown in Fig. 22, where the black dots (●), the white dots (○) and the crosses (×) are the values obtained in Figs. 21 (a), 21 (b) and 21 (c) respectively.

Comparing Fig. 22 with Fig. 18, we can see that these curves agree

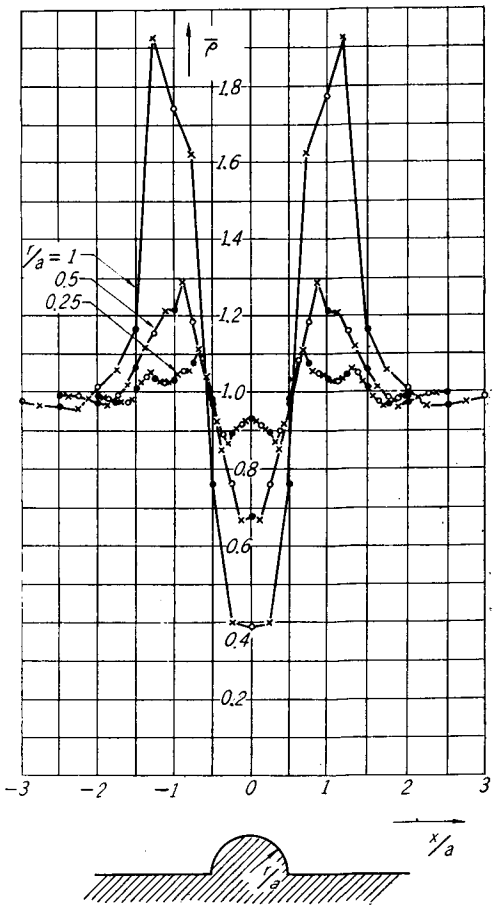

Fig. 22. Resistivity curves.

fairly well with each other, so that it is safe to say that if the length of the radius is more than the net spacing, we obtain resistivity curves which can be considered sufficiently accurate.

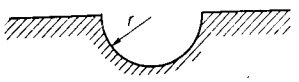

Fig. 23. A hollow of the semi-circular plate section.

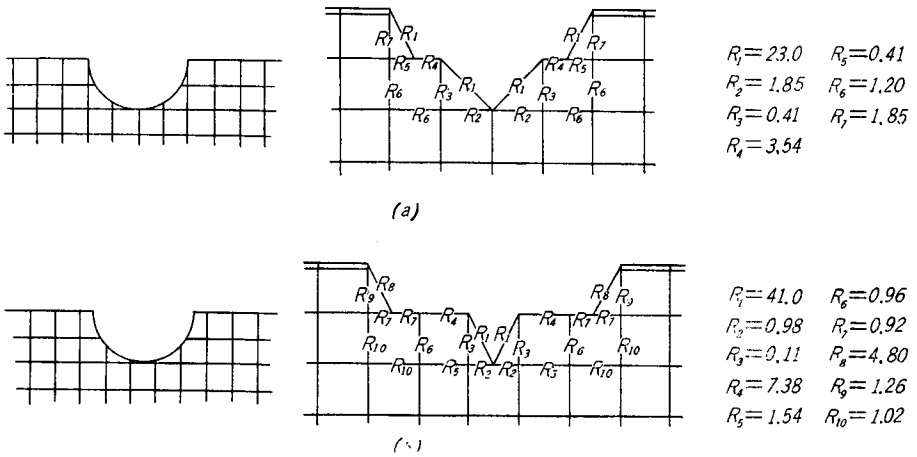

Fig. 24. Center positions and values of the resistors.

4.3 Hollow in the semi-circular plate section (I)

There is a hollow in the semi-circular plate section of which the radius r (as shown in Fig. 23) is twice the net spacing. The center positions and the values of the resistors are shown in Fig. 24. The resistivity curves measured by the analyzer in the above two cases are plotted in Fig. 25, the black dots (●) and the white dots (○) corresponding to Figs. 24 (a) and 24 (b) respectively. In Fig. 25, $a=2$ and 4 correspond to $r/a=1$ and 0.5 respectively. From these curves we can see that the sharp maximum takes place at the center of the hollow in the case of 0.5

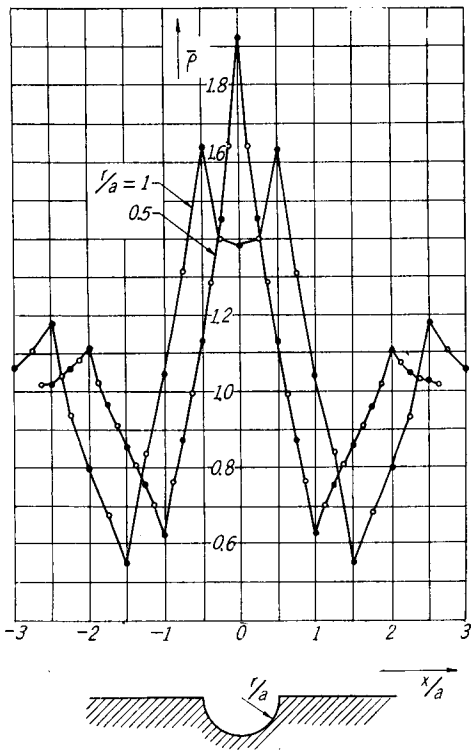

Fig. 25. Resistivity curves.

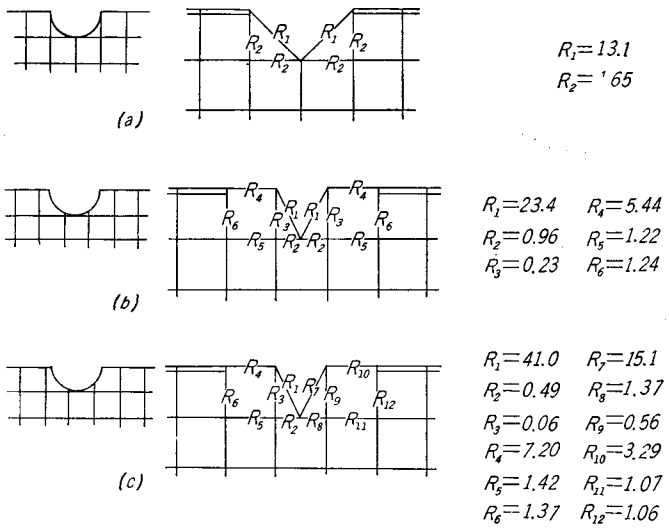

Fig. 26. Center positions and values of the resistors.

and that the minimum takes place in the cases of 2 and 1.

4.4 Hollow in the semi-circular plate section (II)

In a manner similar to section 4.2, we discuss the case in which the radius of the semi-circular plate section equals the net spacing. Figs. 26 (a), 26 (b) and 26 (c) show the three different center positions of the semi-circular plate section and the values of the resistors respectively.

The resistivity curves measured by the analyzer in the above three cases are plotted in Fig. 27, the black dots (●), the white dots (○) and the crosses (×) corresponding to Figs. 26 (a), 26 (b) and 26 (c) respectively. In Fig. 27, $a=1$, 2 and 4 correspond to $r/a=1$, 0.5 and 0.25 respectively.

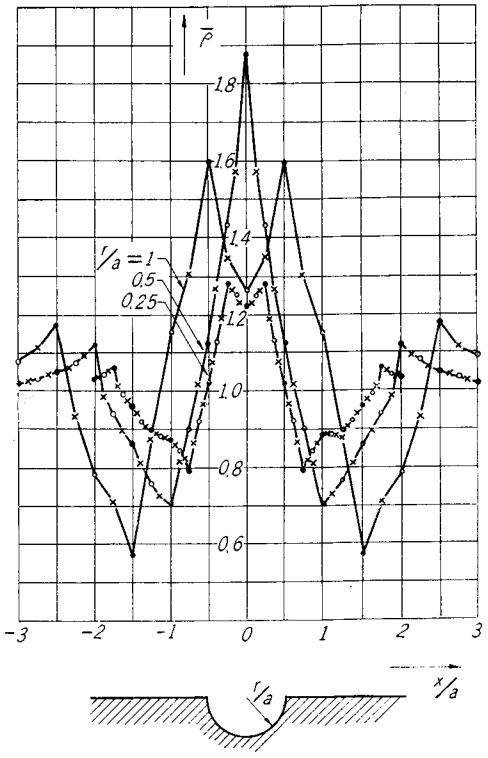

Fig. 27. Resistivity curves.

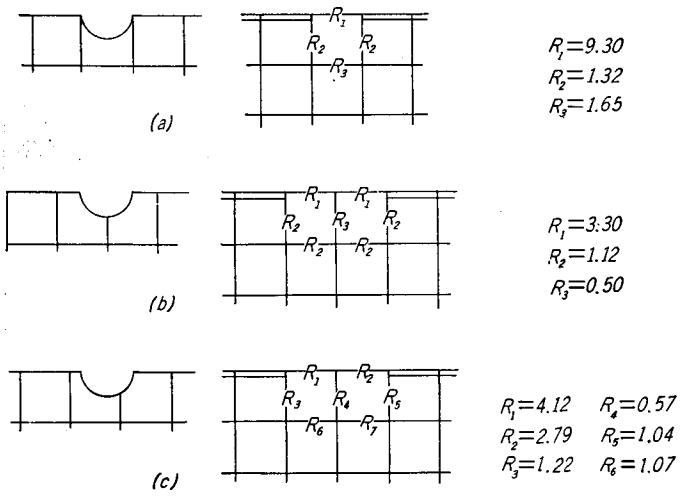

Fig. 28. Center positions and values of the resistors.

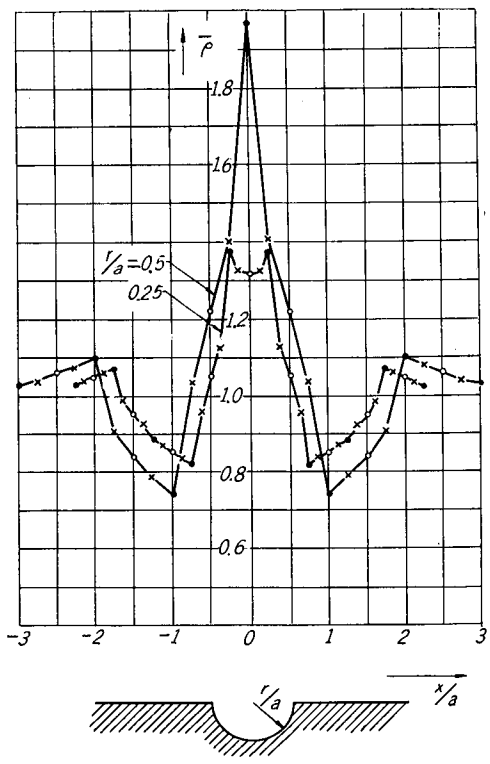

Fig. 29. Resistivity curves.

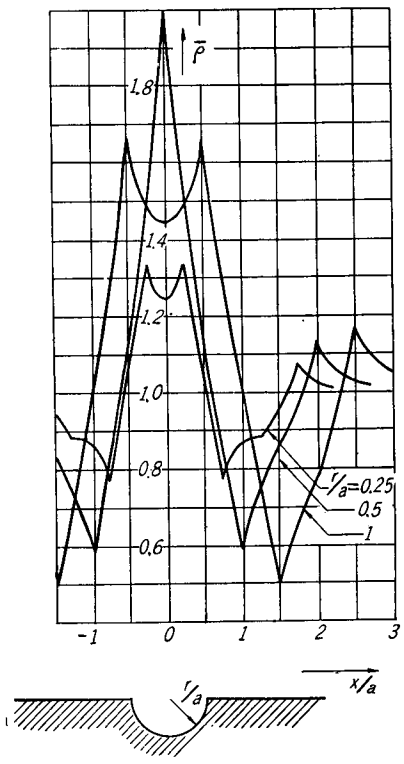

Fig. 30. Theoretical resistivity curves.

4.5 Hollow in the semi-circular plate section (III)

In this section, the radius of the semi-circular plate section is half the net spacing. Figs. 28 (a), 28 (b) and 28 (c) show the three different center positions of the semi-circular plate section and the values of the resistors respectively.

The resistivity curves measured by the analyzer in the above three cases are plotted in Fig. 29, the black dots (●), the white dots (○) and the crosses (×) corresponding to Figs. 28 (a), 28 (b) and 28 (c) respectively. In Fig. 29, $a=1$ and 2 correspond to $r/a=0.5$ and 0.25 respectively. In this case the theoretical resistivity curves are shown in Fig. 30[5].

Comparing these curves with the ones measured by the analyzer, we can see that these curves agree fairly well with each other.

5. Conclusion

In electrical prospecting it is very difficult to solve the general problem of any resistivity distribution, and certain simplifying assumptions are often made about the types of resistivity distributions which occur in practice. Within the limits imposed by these assumptions valuable imformation can sometimes be obtained. But unfortunately, the true resistivity distributions are so complicated that these assumptions can not represent all cases satisfactorily.

It is shown in the present paper that the resistance network analyzer is capable of high accuracy in the solution of Laplace's equations with given boundary conditions.

References

1) E. Yoshizumi and T. Irie; Suiyokwai-Shi, **14**, 54 (1960).
2) E. J. Karplus; Analong Simulation, McGraw-Hill Book Co., (1958).
3) T. Kiyono; Electrical Review, **31**, 673 (1943).
4) N. Kato, Y. Fujita and T. Kiyono; Electrical Review, **30**, 399 (1942).
5) N. Kato, Y. Fujita and T. Kiyono; Electrical Review, **30**, 400 (1942).